Received: 20 June 2022 | Revised: 12 September 2022 | Accepted: 17 September 2022

DOI: 10.1002/bio.4388

REVIEW

LUMINESCENCE WILEY
The Journal of Biological and Chemical Luminescence

High reactive oxygen species produced from fluorescence carbon dots for anticancer and photodynamic therapies: A review

Nurul Mutmainnah Amal[1] | Muhandis Shiddiq[2] | Bidayatul Armynah[1] | Dahlang Tahir[1]

[1]Department of Physics, Hasanuddin University, Makassar, Indonesia

[2]Research Center for Physics, Indonesia Institute of Sciences, Puspiptek, Banten, Indonesia

Correspondence
Dahlang Tahir, Department of Physics, Hasanuddin University, Makassar 90745, Indonesia.
Email: dtahir@fmipa.unhas.ac.id

Funding information
Not applicable.

Abstract

High-photoluminescence carbon dots (CDs) were synthesized from various sources and various methods using two approaches, namely bottom up and top down, with emission-dependent excitation wavelength. Electronic transition from the higher-occupied molecular orbital (HOMO) state to the lowest-unoccupied molecular orbital(LUMO) state, surface defect states, wider excitation spectrum, higher quantum yield, efficient energy transfer, and element doping affected the fluorescence properties of CDs. Using 102 references listed in this review, the authors studied the relationship between fluorescence mechanism and reactive oxygen species (ROS) produced for photodynamic therapy (PDT) and materials anticancer applications. We described how the radical atom or ROS work as anticancer therapy and PDT and described the chemical reaction of high-resolution fluorescence CDs. We summarized experimental techniques that are used for producing CDs and discussed their characteristics. Finally, conclusions and future prospects in this field are also discussed. The important characteristics of CD-based design for high ROS may usher in new prospects and challenges for high efficiency and stability of PDT and anticancer therapy. In conclusion, we have provided perspectives and challenges of the future development of CD s.

KEYWORDS
anticancer, carbon dots, photodynamic therapy, reactive oxygen species

1 | INTRODUCTION

Carbon dots (CDs) are nanoparticles with size 2–10 nm; some studies also reported the CDs' size up to 20 nm when they were combined with graphite and another type of carbon.[1] CDs are nontoxic, naturally available, and inexpensive; CDs can be used in climate analysis, energy storage devices (batteries and capacitors), compound catalysis, electrocatalysis, and photocatalysis.[2]

CDs are carbon-based nanoparticles in the form of carbon nanodots (CNDs), carbon quantum dots (CQDs), and graphene quantum dots (GQDs).[3] GQDs occur in two forms: circles or sheets like graphite. Semicircular nanoparticles with glasslike graphite in the center are called CQDs, which have a delocalized band structure and are potentially modified at the surfaces. Quasi-spherical nanoparticles that do not have complete quantum energy states are called CNDs. Nonetheless, CQDs and CNDs are frequently identified by their characteristics, but the overall properties, including excitation conditions, are difficult to be determined. Therefore, CDs are used to identify all semicircular carbon nanoparticles, which incorporate those with subatomic including delocalized electronic state of all carbon nanoparticles that reach among CND and CQD.[4] GQD is a critical carbon point structure with extraordinary optical and electronic properties, with a

zero bandgap (0 eV) for graphene and up to 3.1 eV for benzene with dimensional change.[5]

CQD performance has been considered the best in various applications as the particles are synthesized by combining two or more methods using different approaches. The bottom-up approach used in synthesizing CDs comprises twist discharge, laser expulsion, and electrochemical oxidation, and the bottom-up approach involves microwave, ultrasonic, solvothermal, and fluid treatments. These synthesized methods can also combine the bottom-up top-down approaches to produce CQDs.[6]

In the bottom-up approach, the hydrothermal method, the most widely used method, applies heat to the fluid containing the carbon source.[7] The CDs are synthesized from a small number of particles using microwave irradiation. The hydrothermal method is used for synthesizing CDs because it is nontoxic and inexpensive and involves a simple procedure. Researchers favor the microwave-assisted technique due to its advantages such as efficient time, low energy, and eco-accommodating nature by carbonization of a small amount of part of plants that are available abundant in nature.[8]

The top-down approach separates the bulk carbon structures using electrolysis, ultrasonic technique, laser ablation, and corrosive treatment. The disadvantages of this approach are as follows: expensive carbon materials, high temperature, harmful natural solvents, and long response time. In addition, this approach can be effectively functionalized using hydroxyl, carboxyl, carbonyl, amino, and epoxy groups on their surfaces and by restricting inorganic and natural sources. The electrochemical method is used to combine pure CDs from large-size atomic matter such as carbon nanotube, graphite, and carbon fiber. Laser ablation has been widely used to synthesize CDs of various sizes. Previous studies[8,9] reported that in laser ablation, complex natural macromolecules formed nanosized carbon particles under laser irradiation.

Zhou et al. reported the synthesis of CDs from multiwalled carbon nanotubes in the presence of tetrabutylammonium perchlorate as electrolyte.[10] Xu et al. reported the synthesis of CDs from single-walled carbon nanotubes (SWCNTs) using the arc discharge method.[11] In 2009, Zhu et al. reported the synthesis of CDs from carbohydrates with excellent photophysical properties in a short reaction time.[12]

The aim of this article is to describe the synthesis and properties of CDs. The main characteristic of CDs is photophysical property, especially fluorescence that results from surface functionalization with solubility in aqueous and nonaqueous solutions.[13] The fluorescence of CDs was reported from the deep-blue (430 nm) to the near-infrared (NIR, 730 nm) regions, which highly correlated with the bandgap.[14] The quantum yield (QY) of CDs is generally low, and it is increased usually by functionalization of phenolic compounds and the atoms present in the plant extracted. The surface state at the outer layer of CDs has an energy level and leads to different emission, which is also similar for the subatomic state. The reaction at the atomic state occurred in aqueous solution via bandgap when absorbing a photon ($h\nu$) in producing the reactive oxide, which is important for anticancer and photodynamic therapy (PDT).[15] The oxidation at the surface state increased when the bandgap decreased, which affected the number of reactive oxides produced.[16] First, the CDs absorbing the photon and the electron (e^-) at the higher-occupied molecular orbital (HOMO) state have energy to jump to the lowest-unoccupied molecular orbital (LUMO) state and remain as a hole (h^+).[17] Second, the e^- at the HOMO will react with O_2, and the h^+ at the LUMO will react with H_2O.[18] The reactions of both processes will produce the reactive oxide in the form OH*, which is useful for the next reaction for anticancer therapy and PDT:

$$\mathrm{CDs} + h\nu \rightarrow e^- + h^+ \quad (1)$$

$$O_2 + e^- \rightarrow {O_2}^{*-} \quad (2)$$

$$H_2O + h^+ \rightarrow H^+ + OH^* \quad (3)$$

$${O_2}^{*-} + H^+ \rightarrow H_2O^* \quad (4)$$

$$H^+ + H_2O^* \rightarrow H_2O_2 + e^- \rightarrow OH^- + OH^* \quad (5)$$

$$OH^- + h^+ \rightarrow OH^* \quad (6)$$

These species may affect downstream reactive oxygen species (ROS) such as the H_2O^* radical and hydrogen peroxide (H_2O_2). For considering ROS as being oxygen dependent, the OH* radical must also be produced by the reaction.

The emission of CDs may result from surface state emission, intrinsic band emission, triple ground state emission, dipole emission involving electron–phonon coupling, transition from HOMO to LUMO, self-trapped excitons, and presence of small organic molecules. The excitation-dependent emission is typically attributed to the presence of multi-emission centers, size distribution, solvent relaxation, and existence of multi-aggregation.[8,9] The optical properties of CDs are strongly dependent on the local environment, surface structure, and electron transfer from the CDs to other species.[10,11]

For electron–hole annihilation and radiative recombination usually occured by direct luminescence emission.[19] Several groups reported the luminescence mechanism of metal-based and nonmetal-based CDs.[20] They also reported the luminescence reaction between CDs and H_2O_2 or the mixing system with additional ${HCO_3}^-$.[21] The unstable intermediate reaction resulted in $1O_2$ and $(O_2)_2{}^*$ to produce luminescence emission. The ROS was produced from the reaction between ${HCO_3}^-$ and H_2O_2 to form hydroxide radical (OH*) and superoxide ion radical (${O_2}^{-*}$), which is described as follows:

$$H_2O_2 + {HCO_3}^- \rightleftharpoons {HCO_4}^- + H_2O \quad (7)$$

$${HCO_4}^- \rightarrow OH^* + {CO_3}^{-*} \quad (8)$$

$$H_2O_2 + {CO_3}^{-*} \rightarrow {HCO_3}^- + {HO_2}^* \quad (9)$$

$$HO_2^* \rightarrow O_2^{-*} + H^+ \quad (10)$$

$$O_2^{-*} + OH^* \rightarrow 1O_2 + OH^- \quad (11)$$

$$O_2^{-*} + HO_2^* \rightarrow 1O_2 + HO_2^- \quad (12)$$

$$HO_2^* + HO_2^* \rightarrow 1O_2 + H_2O_2 \quad (13)$$

$$1O_2 \rightarrow 3O_2 + h\nu \quad (14)$$

$$2O_2^{-*} + 2O_2^{-*} + 4H_2O \rightarrow (O_2)_2^* + 2H_2O_2 + 4OH^- \quad (15)$$

$$(O_2)_2^* \rightarrow 2O_2 + h\nu \quad (16)$$

$$OH^* + HCO_3^- \rightarrow HO^- + HCO_3^* \quad (17)$$

$$2HCO_3^* \rightarrow H_2O_2 + (CO_2)_2^* \quad (18)$$

$$(CO_2)_2^* \rightarrow 2CO_2 + h\nu \quad (19)$$

The intermediate radicals OH*, CO_3^{-*}, and O_2^{-*} react with CDs that are produced from H_2O_2 or mixing system with HCO_3^- to generate positively (CDs^{+*}) or negatively (CDs^{-*}).[22] The CDs exhibited strong luminescence emission when the excited state of the positive or negative CDs* was returned to ground state.[21] These radicals are important for anticancer therapy and PDT.

This review aims to systematically discuss how radical atoms work in anticancer therapy and PDT and describe the chemical reaction of high-resolution fluorescence CDs. We first introduce ROS in general and summarize the experimental techniques that are used to produce high-luminescence CDs. We then present the synthesized methods used to fabricate CDs and discuss their characteristics. The last two sections discuss anticancer therapy and PDT as promising applications of CDs. In conclusion, we provide an outlook on CDs, introducing perspectives and challenges of the future development of CDs.

2 | SYNTHESIZED CDs

There are many sources of carbon in nature, for example, parts of plants. CDs are synthesized using two approaches: top down and bottom up; these are highly correlated with CD performance. Different types of CDs can be extracted from different carbon forms, including graphite, graphene, carbon nanotube, fullerene, coal, black carbon, and activated carbon. The synthesis methods strongly depend on the type or condition of precursor or sources of CDs using laser ablation, mechanical milling, chemical oxidation, electrochemical oxidation, arc discharge, and ultrasonic-assisted techniques. The hydrothermal method is used for the development of CDs from a little carbon moiety, which is similar for microwave-assisted techniques, plasma treatment, pyrolysis, and ultrasonic reaction.[23]

The synthesis methods can be selected based on comparative feasibility, targeted application, and desired properties. For example, the top-down approach is easy to produce, simple and well structured, whereas the bottom-up approach is difficult due to the formation of various side products along with CDs.[24]

The uniformity arrangement of CDs particle synthesized by the hydrothermal/solvothermal method was affected by the high temperature and high fume pressure during synthesized processes.[25] The hydrothermal technique has become one of the most standard strategies to integrate graphene CDs for high QY.[26] The hydrothermal conditions such as water properties, consistency, fume pressure, surface strain, and ionic item are essentially changed. High temperatures (in the range of 300–800°C) result in high carbon content materials such as carbon nanotubes and graphitic carbon.[27] In 2011, Zheng-Chun reported the hydrothermal glucosamine hydrochloride method for producing nitrogen-doped CDs with size 15–70 nm at 140°C for 12 h. During hydrothermal treatment dehydration, polymerization, and nucleation of glucosamine molecules with aromatic amine, hydroxyl, and carboxyl groups on the surface of CDs with fluorescence at 510 nm. Typically CDs synthesized at high temperature consequently incur extra cost for the process. The combination of synthesizing methods will reduce the processing temperature to room temperature with the assistance of oxidizing agents. Hydrogen peroxide is one oxidizing agent that converts hydroquinone to *p*-benzoquinone, and the exothermal response is used to carbonize and produce photoluminescence (PL) CDs at room temperature.[28]

It has been determined that microwaves comprise long-frequency electromagnetic waves.[29] This technique is exceptionally productive with high yields, specificity, cost effective, simple, fast, and energy saving; has short response times, controlled temperature, controlled size, security, and better reproducibility, and; and causes low pollution.[30] The microwave strategy can adequately reduce the response time and provide uniform, homogeneous heating, resulting in uniform-sized CDs. In 2016, Mehta reported using the microwave method for synthesizing CDs from sugarcane syrup with an orange particles that contained carbon and nitrogen in the form of GCDs (size 2–6 nm) and green fluorescence at wavelength 254 nm.[31] CDs from l-asparagine were reported by Wang et al. with a microwave temperature of 180°C for 15 min.[32]

Pyrolysis was reported for producing QDs[33] but was not widely used as this technique required high temperature and high energy. Devi et al. reported utilizing *Aloe vera* extract that was exposed to a high temperature of 160–250°C for 10–30 min for carbonization. This technique resulted in the production of CDs with a QY of 12.3% and showed the emission under UV light due to excitation, as seen in PL, UV spectroscopy, Fourier-transform infrared spectroscopy (FT-IR), and Raman spectroscopy. The CDs from *Aloe vera* exhibit antibacterial properties for detecting metal particles.[34] The study reported by Ubani et al. combined CdSe and QDs using pyrolysis for organometallic reagents. The combination was completed for cadmium oxide arrangement using pyrolysis at 195°C to deliver discrete homogeneous nucleation with dissimilarities in nanocrystal size and shape.[35]

The ultrasonic technique has benefits such as green synthesis method, cost-effectiveness, strong penetration, and uniform particle distribution.[36,37] The QY of CDs by this technique could be increased from 3.3% to 28.3% compared with other methods which have great scattering properties, low crystallinity, and useful state at the surface.[38]

For the microwave-assisted technique and the ultrasonic waves, high-energy for synthesized pure CDs and doped-CDs was used as reported in 2020 by Gao et al.[39] The mixing N, S, P as a co-doped CDs (N, S, P-CDs) at room temperature shows effectively applied for antibiotic medication mixed with milk.[39] Laser ablation was used direct UV-pulsed light to produce CNDs which different with electrochemical methods by voltage contrasts between anodes in an electrolyte of water and ionic fluid. This methods more safety because no harmful gas used in synthesizing and easily produce uniform distribution of CDs in ionic fluid-free electrolyte.[40]

Laser ablation is an efficient physical method that irradiates a solid target in liquid[41] to produce CDs. Huang et al. was reported using Nd:YAG laser (1064 nm, 10 Hz) for carbon target through water bubbler from argon gas at 900°C and 75 kPa.[42] For laser ablation, the time and the wavelength laser is important parameters for controlling the CDs characteristics.[43] In 2016, the impact of laser frequency on ablation cycle was reported that affect to the optical properties of CDs from three different frequencies: 1064, 532, and 355 nm of the Nd:YAG laser.[44]

Wet chemical techniques or chemical oxidation usually used semiconductor as a doping, such as Si/Ge QD.[45], or H_2SO_4 or mixed oxidative with HNO_3 can also be used. This technique was used to produce various ROS or oxygen atoms in the form of −COOH and −OH.[46] The methods for increasing ROS were reported by Gaponik et al. who synthesized it using the wet-compound combination technique from thioglycolic acid (TGA) covered by CdTe in the form of CdTe-QDs.[47] Figure 1 shows the number of publications using various synthesized CDs methods. The synthesis method using the bottom-up approach is indicated by blue color, whereas the top-down approach is indicated by red color. Globally, scientists synthesized a large number of CDs using the microwave and hydrothermal methods as they are simple and efficient.[48]

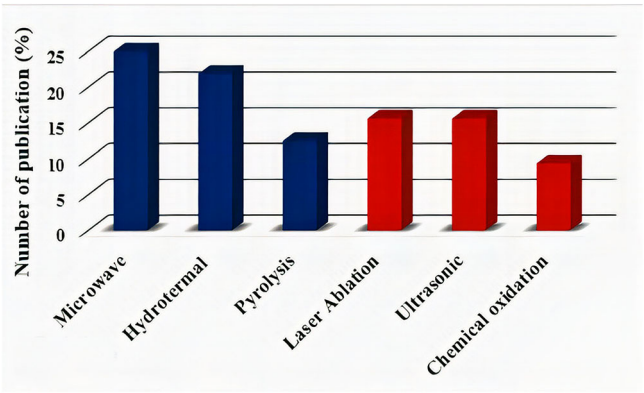

FIGURE 1 Number of publications reported by scientists for synthesizing CDs using the bottom-up (blue color) and top-down approaches (red color)

3 | METHODS

The Preferred Reporting Items for Systematic Reviews and Meta-Analyses (PRISMA) standards were followed for conducting this systematic review. A systematic search of the CD database for PDT and anticancer therapy by evaluating article titles, abstracts, and full texts and data extraction process is shown in Figure 2.

3.1 | Literature search and selection strategy

ScienceDirect (sciencedirect.com) was used to search articles for analysis using keywords "carbon dots," "fluorescence carbon dots," "carbon dots for photodynamic therapy," and "carbon dots for anticancer." There were no regional or chronological limits to the search results. Several titles and abstracts that could be potentially useful were identified through a manual check. All relevant articles were manually examined. They were downloaded; then the titles and abstracts were read and categorized into folders named high, medium, and low correlation. Those papers that had no correlation with PDT and anticancer therapy were deleted from the folder. We also excluded book chapters and mini reviews; Figure 1 and Table 1 present more details.

3.2 | Data extraction and critical appraisal

The following sources of CDs were recorded from each article: citric acid–doped urea, citric acid–doped tryptophan, citric acid–doped RNase A, *Hypocrella bamboosae* (*HB*), glycerol, carrot, persimmon fruit, mulberry leaves (*Morus alba* L.), Radix Puerariae, CDs coated with titanium dioxide (TiO_2), Eudragit RS 100 CDs, bamboo leaf, *O*-carboxymethyl chitosanprocaine, citric acid, and ethylenediamine. The various synthesized methods are microwave technique, microwave-assisted pyrolysis, solvothermal technique, hydrothermal technique, pyrolysis, and ultrasonic technique. The last technique provides the percentage of the QY for PDT and anticancer therapy, as presented in Table 1.

3.3 | Statistical analysis

The data were qualitatively synthesized, with total numbers and percentages used when applicable.

Table 1 presents the CDs produced using the bottom-up and top-down approaches, including size, and QY, which were synthesized from various sources and methods for PDT and anticancer applications of CDs. The number of publications on anticancer therapy is

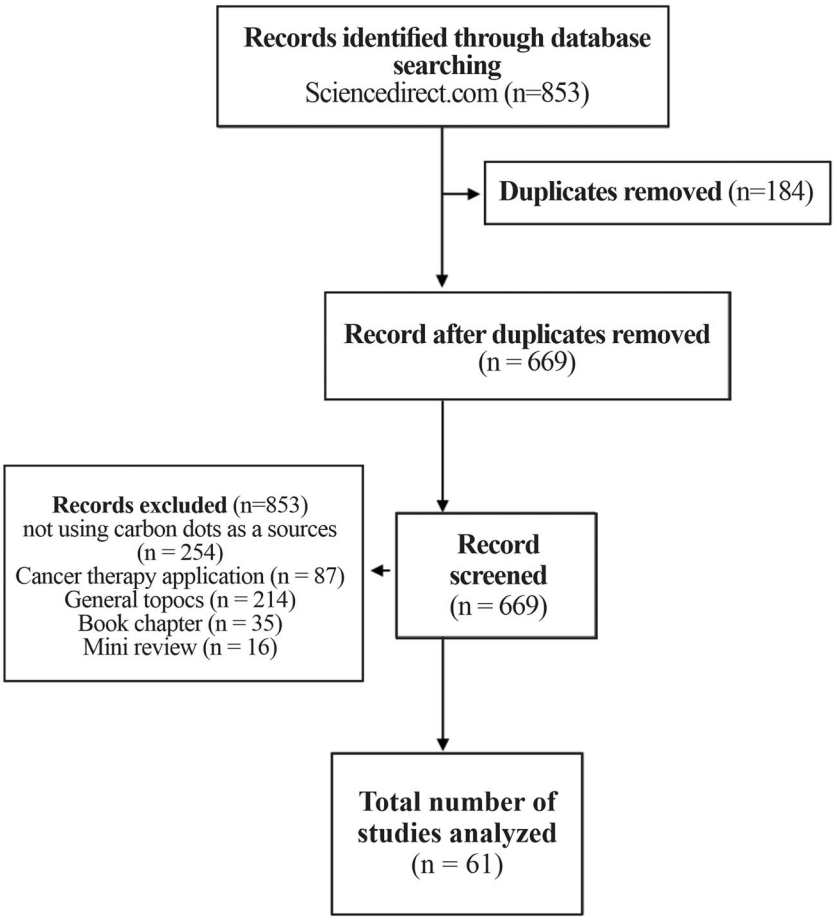

FIGURE 2 PRISMA (Preferred Reporting Items for Systematic Reviews and Meta-Analyses) diagram demonstrating the full-text article selection process

TABLE 1 Methods of synthesis of CDs from different sources and their relative size, quantum yield, and applications for photodynamic and anticancer therapies

Sources	Methods	Size (nm)	Quantum yield (%)	Applications	Reference
Citric acid, boric acid, urea	Microwave	2–6	10–15	Photodynamic therapy	[49]
Citric acid, tryptophan	Microwave-assisted pyrolysis	2–6	54		[50]
Citric acid, RNase A	Microwave	25–45	24.20		[51]
Hypocrella bambusae	Solvothermal	–	0.38		[52]
Glycerol	Microwave pyrolysis	9 ± 1.1	–	Anticancer	[53]
Carrot	Hydrothermal	2.30	7.60		[54]
Persimmon fruit		5.2 ± 1.7	14.9		[55]
Mulberry leaves (*Morus alba* L.)		2–4	–		[56]
Radix Puerariae	Pyrolysis	1.0–8.0	54		[57]
CDs-coated titanium dioxide (TiO_2)	Hydrothermal	4–27	–		[58]
Eudragit RS 100 CDs		50	–		[59]
Bamboo leaf	Ultrasonic	0.24	–		[60]
O-Carboxymethyl chitosan		4.5 ± 10	–		[61]
Procaine, citric acid, and ethylenediamine	Hydrothermal	2–5	47.1		[62]

larger than that on PDT, which may be due to the characteristics of CDs, including environment friendly, biocompatible, broader excitation spectra, better photostability, size-dependent emission wavelength, higher QY, and efficient transfer energy. The additional metal in CDs was usually used to produce high ROS systems for anticancer therapy and PDT.

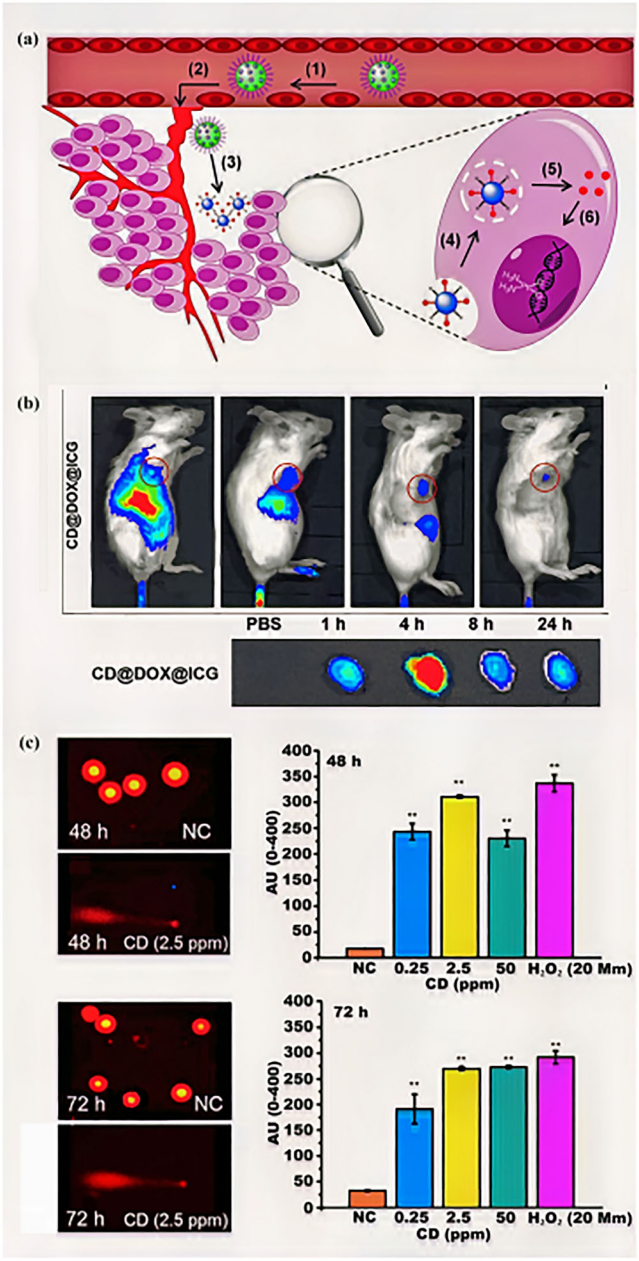

FIGURE 3 (a) Schematic illustration of drug delivery of CD-doped metal and polymer for anticancer therapy[63]; (b) fluorescence intensity of kappa, folic acid (FA), and carrageenan (KFC-CDs) injected in mice for control (PBS) and treated for the period of identification up to 24 h[64]; (c) representation of the different CDs in the alkaline assay where MCF7 cells were visually scored for 48 and 72 h for different CD concentrations (ppm)[65]

4 | FLUORESCENCE FOR ANTICANCER THERAPY

Tao Feng et al. reported the CD-based drug nanocarriers that are advantageous, when compared with conventional nanocarriers, including (1) negative charge/PEGylation to prolong blood circulation time, (2) accumulation at tumor sites because of increasing permeability and retention, (3) increased internalization of tumor cells due to load-modifiable properties in the tumor extracellular microenvironment, and (4) fewer side effects under normal physiological conditions. The CD-based drug nanocarriers exhibit improved tumor inhibitory activity and reduced side effects, indicating high potential for cancer therapy (Figure 3).[63,66]

Poushali Das et al. reported that there is no significant change in emission intensity when KCl content increased from 0 to 2.6 M but varied salt concentrations for fluorescence-based sensing applications of kappa, FA, and carrageenan (KFC-CDs). KFC-CDs have stability and steady fluorescence for pH in the range of 5.1–9.7and for various environmental conditions with 0.15 mM NaCl and 10 mM Tris–HCl. The photostability of KFC-CDs is continuous at a wavelength of 365 nm using UV irradiation with stable fluorescence up to 95 min. The photoluminescent properties of KFC-CDs in aqueous solution show stronger resistance to photobleaching compared with that of the commercial organic dye.[64]

The CDs effectively damage cells compared with untreated cells; the Arbitrary Unit (AU) value was twice for the lowest CD concentration (0.25 ppm). The surface charge and surface functional groups affected the interaction between CDs and cells to induce DNA damage and failed to repair due to oxidative stress, causing genomic instability. The CD surface functional group was determined using FT-IR and X-ray photoelectron spectroscopy (XPS) to identify the oxygenated functional groups used for synthesis of ROS. Sarkar et al.[67] reported ROS generation using CDs by manipulating oxygenated groups from carboxyl groups. The higher oxygenated groups on the surface of CDs are affected, the higher the ROS production capacity.

The characteristic ligand on the surface CDs in the form of the oxygenated group has high affinity and flexibility for surface modification. Ligand–receptor interactions are important for targeting antigens–antibodies for localization of sick cells in different tissues that work intracellularly.[68] Biosensors have been developed from CDs by hydrothermal from ammonium chloride and QDs from CdTe by sealing with n 3-mercaptopropionic acid show that can be used for detection of HIV-DNA in biological samples.[69]

Fahmi et al. reported that natural CDs, synthesized from bamboo leaves (0.24 nm), have proven useful for delivering anticancer drugs to the target cancer cells. Fluorescence and cellular pathways were analyzed using in vitro confocal microscopy.[60] Similarly, Reddy, in 2020, synthesized CDs from persimmon fruit using the hydrothermal method with a size of 5.2 ± 1.7 and QY of 14.9%.[55] The CDs on coprecipitation with the rutile phase of TiO_2 nanoparticles were investigated by Sawant et al.[58] by modifying surface engineering, which can minimize the hydrophobicity of curcumin and increase its biocompatibility. The anticancer potential for breast cancer cells is higher for CD-coated TiO_2 nanoparticles compared with that of CDs without TiO_2 coating.[70]

The anticancer capability of CDs should be high optical luminescence usually used synthesized from various flavors of red stew, turmeric, dark pepper, and cinnamon with high QY of 43.6%.[71] As reported by Cutrim et al., ESM 2021 the nanofabrication of anticancer from the outer layer of CQDs glasslike structure from hydroxyl, carbonyl, carboxylate, and carboxylic amines. The connection at the

surface of CQDs is electrostatic of hydrogen atoms as nano conjugates to build the bonding with atom from cell diseases.[72]

5 | FLUORESCENCE FOR PDT

The carbon nitride in CDs was used to improve ROS generation[73] for PDT using a metabolic mixed prodrug for a certain frequency of light. In this treatment, the photochemical and photobiological activities damage the growing tissues. Preclinical and clinical studies reported and confirmed the possible photodynamic treatment to be used as therapeutic methods for malignant growth.[74] Nanocomposites of CDs also induce tumor hypoxia and increased anticancer activity.[72] PDT is a noninvasive therapeutic procedure using natural photosensitizer (PS) particles to absorb light for exciting the charge and increasing the ROS species.[75]

PDT is a nonsystemic treatment involving three nontoxic components used in combination: the light-activated PS, a specific light source, and ROS. The interaction between the light with CDs for the right wavelengths and dosage in the PS system through chemical reactions is described in the Introduction. The electron transfer from the PS system to the substrate molecules produces free radicals and radical ions. The energy transfer from the PS to the molecular oxygen produces singlet oxygen species ($^1O_2$), as shown in Figure 4a, for the primary process in PDT, as reported by Qingyan Jia et al. for *HB* which is a parasitic fungus found in bamboo. Photodynamic antiviral and anticancer properties of hypocrellins isolated from *HB* have been demonstrated[78,79] using CDs from *HB* synthesized using solvothermal methods called HBCDs, as shown in the upper part of Figure 4(b). The HBCDs have high water solubility, wide absorption, red-light emission, and biocompatibility, which was used to guide cancer treatment for fluorescence and photoacoustic imaging agents. The HBCDs efficiently produce ROS, specially $^1O_2$, which is used in hyperthermia by PDT as an effective anticancer therapy. The CDs containing natural biomass as the raw carbon source such as HBCDs show bifunctional fluorescence and photoacoustic imaging with synergistic PDT for cancer treatment.[52]

The fluorescence imaging was performed in PDT to illustrate the capacity CDs- Ce6's in vivo for theranostics applications in subcutaneous MGC803 gastric cancer xenograft in animal model. The mice (with tumor size of 25–30 mm) were administered C-dots-Ce6 intravenously, and the PDT process was monitored in vivo via NIR fluorescence imaging. The light emitted from the CDs-Ce6 is clearly observed in the tumor location in Figure 4(c), indicating high fluorescence intensity.[76]

Recently, Xiaolong Hu et al. reported their findings regarding CD-based Sn nanocluster with a high QY of 58.3%. The PDT test used the HepG2 cell model before examining the biological applications of CD-based Sn nanocluster. The living cells are indicated by green color and dead cells by red color for irradiation wavelengths 490 and 545 nm. Figure 4d) clearly shows strong green fluorescence and red fluorescence in HepG2 cells using CDs-based Sn nanocluster for dark and light conditions.[77]

PDT is a promising noninvasive cancer treatment used in combination with surgery, chemotherapy, or ionizing radiation to destroy

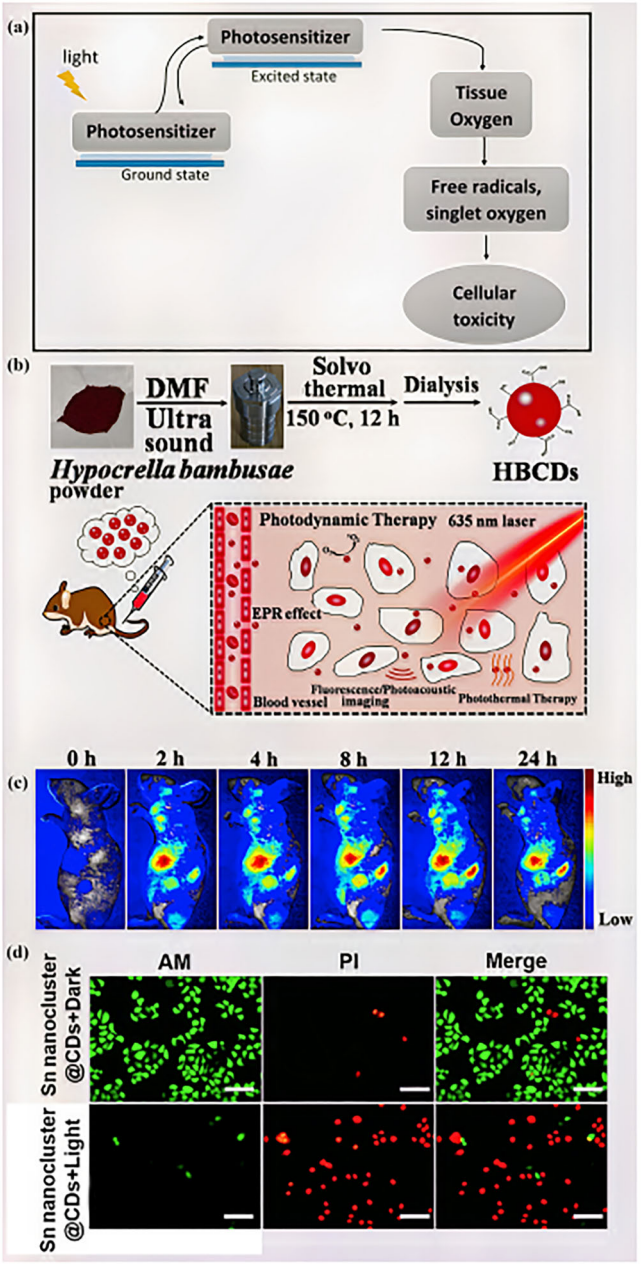

FIGURE 4 (a) Illustrative procedure for producing ROS (reactive oxygen species) when light coming to the CDs is photosensitized in the process of photodynamic therapy (PDT), (b) schematic illustration of HBCDs derived from *Hypocrella bambusae* by solvothermal method in blood vessel imaging and synergistic PDT of cancer using 635-nm laser,[52] (c) real-time NIR (near infrared) fluorescence images after intravenous injection of CDs-Ce6 at different times up to 24 h with focus points of the average fluorescence intensities from the tumor area,[76] and (d) microscopy images of living HepG2 cells (green, 490-nm excitation) and dead cells (red, 545-nm excitation) after treatment with 250-mg/ml Sn nanocluster@CDs solutions in additional dark and light conditions.[77]

undetected cancers cells.[80] PDT uses photosensitizing drugs of pharmacology with a particular light wavelength irradiation for the presence of ROS to induce cell death and tissue necrosis,[81–83] as shown in Figure 4(b).

Huang et al.[76] reported the theranostic system based on chlorin e6–conjugated CDs (CDs-Ce6) that exhibited good stability and solubility, low cytotoxicity, good biocompatibility, enhanced photosensitizer fluorescence detection (PFD), and very good photodynamic efficacy. The results suggested that the new synthesized system exhibited excellent imaging and tumor-homing ability, excellent photodynamic efficacy, and effectiveness in simultaneous PFD and PDT. In 2015, a study reported the in vitro and in vivo effects of a transdermal CDs-chlorine e6-hyaluronate (CDs-Ce6-HA) conjugate for PDT of melanoma skin cancer and showed significant photodynamic effect on cancer cells of melanoma skin cancer.[84]

Ge et al. synthesized 2–6 nm GQDs and exhibited their high performance in ROS generation, indicated by reduction in tumor size in a 17-day treatment.[85] Tabish et al. reported GQDs with a size of 20 nm and a QY of 7.1%, showing high ROS generation for irradiation at 365 nm.[86] Campbell et al. synthesized GQDs using three covalently bounded components, namely nitrogen-doped GQDs, hyaluronic acid, and ferrocene, and showed high (thrice) ROS generation compared with pure ferrocene.[87] The doping sulfur and nitrogen atoms of GQDs show improved phototherapy performance due to nitrogen bonding that increased ROS generation compared to single GQDs.[88,89]

The antitumor nature of CDs based on PDT has been confirmed by Li et al. using porphyrin-containing CDs and shows effective photodynamic activity against hepatoma due to its ability to suppress the tumor mass.[90] Huang et al. reported the theranostic system used on chlorin e6-conjugated CDs and showed high photodynamic efficacy, compared with that of pure Ce6, and good imaging efficacy.[76] Qin et al. reported using microplasma for synthesizing CDs with absorption peak between 380 and 500 nm and emitting strong yellow fluorescence at 550 nm. HeLa cancer cells quickly absorbed the CDs when activated under blue light; a yellow fluorescence and ROS were produced effectively, allowing for simultaneous fluorescent cancer cell imaging and photodynamic inactivation, with a 40% reduction in relative cell viability.[91]

PDT is used to treat lung and gastrointestinal malignancies due to the ROS in the form of singlet oxygen, which depends on energy. Cells in contact with the PS, light, and oxygen simultaneously show cytotoxic responses. The fluorescence occurred from the energy transfer device of quantum dots to the silicon Pc4 PS to produce ROS for PDT as reported in earlier research.[92,93] Song et al. developed polyvinylpyrrolidone-modified zinc oxide QDs with high PL and a strong inhibition for tumor cells[94] and also new cationic porphyrin PDT medicines for cancer using GQDs.[95]

6 | OPTICAL PROPERTIES OF CDS FOR ROS GENERATION

Light wavelength effectively activates the PS to generate ROS, which corresponds to the electronic absorption band of CDs. Light interaction with tissues results in four physical phenomena: absorption, scattering, transmission, and reflection,[96] as shown in Figure 5(a) (three dimensional)[97] and Figure 5(b) (two dimensional).[98] Penetration depth and efficient delivery of light are two important parameters for deep tissue treatment and generation of ROS for anticancer therapy and PDT. These parameters are dependent on the wavelength of light, for UV–Vis. penetration was limited only from the epidermis through the dermis, but X-rays penetrate the hypodermis.

The parameter for light penetration into tissues depends on the light or photon energy, optical properties of tissues in the form of refractive indexes and extinction coefficient, polarization, coherence, power density, irradiation time, and tissue physiology such as pigmentation and hydration.[99,100] Endogenous fluorophores, including hemoglobin and melanin, have strong absorption in the visible light at a wavelength <630 nm. Therefore, an absorption peak must form in the wavelength region of 630–700 nm to maximize tissue penetration and high ROS generation.[101] The NIR will be absorbed by water and lose its energy with increasing wavelength, but optimum deep tissue penetration should be in the range of 700–1000 nm.[102]

At low energy, light in the wavelength >850 nm is relatively very low, and ROS generation is due to the thermal effects from fast nonradiative transitions and narrow bandgap energy.[103,104] Shorter light wavelength will be scattered by the tissue and has limited transmission. Therefore, PSs that absorb red or NIR photons in the wavelength between 650 and 850 nm have high potential to effectively penetrate tissues.[105,106] The physical phenomenon by scattering and reflection of light is challenging for PDT application. This physical phenomenon may not allow the photons to reach all parts of the irradiated area. To generate ROS in the irradiated area such as tumor tissue, an accurate irradiation margin must be considered for thicknesses of 3–4 mm.[107]

The increasing number of new PSs for PDT application has led to a breakthrough in photomedicine. The development of PDT agents has improved most of the characteristics, although the widely used Photofrin has several disadvantages such as low light absorption and poor light penetration, poor clearance from the body, and prolonged photosensitivity. PSs include specifically targeted antibodies, serum albumin, sugars, peptide ligands, and nonprotein ligands to increase phosphorothioate (PS) accumulation in cancer cells and bind with proteins.[108,109]

The depth of light penetration into tissues depends on the optical properties of the tissues and the wavelength of light. The endogenous pigments hemoglobin and melanin absorb shorter wavelengths, thereby affecting light transmittance.[110–112] The light within the spectral range 600–1300 nm called "phototherapeutic window" is critical for PDT.[113] Light with wavelengths in the range of 620–850 nm has the most penetrating ability. Above 850 nm, light does not have sufficient energy for activating PS; consequently, PS cannot generate sufficient energy to produce singlet oxygen. The light within the wavelength of 620–850 nm is the optimum wavelength that can penetrate maximum tissues for PDT applications.[114] The light source used for PDT has some unique properties. First, the determination of light depends on the type of disease such as tissue type, tumor location, and size. Next, the light source suitable for PS absorption should be used.

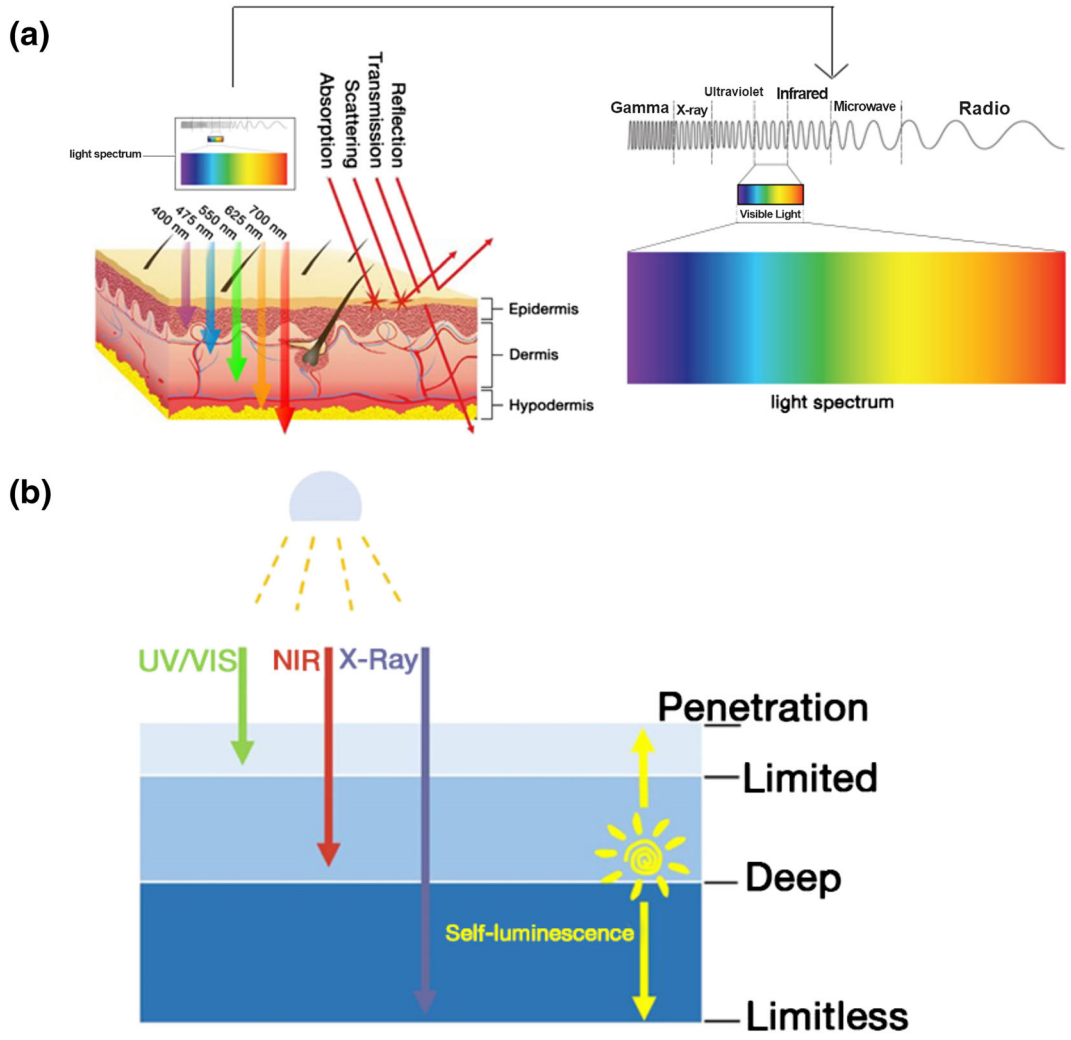

FIGURE 5 (a) Illustrative procedure of light interaction with human tissues.[97] (b) Two-dimensional interaction for various light energies or wavelength and their penetration abilities.[98]

The power and density of the light delivered are also important for the light source, that is divided into coherent and noncoherent properties for PDT application. The coherent light sources are argon-pumped lasers, solid-state lasers, metal vapor–pumped dye lasers, and optical parametric oscillator lasers. Noncoherent light sources are fluorescent lamps, halogen lamps, metal halide lamps, xenon arc lamps, and phosphor-coated sodium lamps.[115] For superficial lesions such as skin and oral cavities, noncoherent light sources may be used, because they are cost effective and commercially available, compared to laser. Moreover, they can be used for various PSs because of their broad emission range.[114] Coherent light in the form of lasers is widely utilized in devices for clinical applications of PDT because of the monochromatic coherent light with very high output. Therefore, the time required to apply PDT can be reduced.

To optimize the light source for PDT, the LED-based PDT provides many advantages: inexpensive, easy to design, and large irradiation field.[116–118] A narrow emission band can be selected to maximize the PS effect compared to using daylight.[119] It is known that daylight cannot penetrate deep tissues, and the emission spectrum contains blue light that is effective for superficial treatments such as nonmelanoma skin cancer and actinic keratosis.[120]

Penetration depth of X-rays may usher in new methods to achieve efficient PDT of deep-seated tumors.[121,122] High X-ray photon energies (from keV to MeV) are not available in conventional PS for singlet–triplet energy gap. Therefore, X-ray singlet–triplet energy gap requires energy mediators such as scintillating nanoparticles (SCNPs). SCNPs can convert high-energy ionizing radiation into UV–Vis. light via a three-step scintillation process near PS.[123–125] Using SCNPs, X-rays as an excitation source make it possible to achieve high ROS generation and superior therapeutic efficacy for PDT.

PDT plays an important role in the treatment of malignancies with noninvasive and photothermal coupling agents required for PDT implementation.[126] DOX loaded with SWCNTs-PEG-Fe3O4@CQDs potentials destroys cancer cells by releasing ROS photodynamically or

photothermally and converts to heat energy to kill cancer cells. The SWCNT-PEG-Fe3O4@CQD nanocarriers are ideal for treating cervical cancer and other disorders.[127]

CQD nanocomposite has been reported to deliver the drug to kill cancer cells by functionalized FA and conjugated with a riboflavin PS. Cross-linked chitosan complexes (Ch-Fe-CL) are used as precursors for synthesis. CQD nanocomposites were doped with FeN to form FeN@CQDs and incorporated into polymer nano-spheres to be applied to chemotherapeutic molecules (DOX). These nanocomposites show strong NIR absorbance with high-efficiency photothermal conversion. NIR light stimulates the drug and allows it into cell to kill cancer cells.[128] CQDs and C60 fullerenes were reported to be used as PS drugs with high ROS to detect photodynamic cytotoxicity.[89]

In 2015, A.B. Bourlinos used the microwave method to synthesize citric acid–doped boric acid as the CD source with a size of 2–6 nm and a QY of 10%–15%.[49] Similar results were reported in 2014 by Q. Wang. Q. Wang succeeded in synthesizing tryptophan-doped citric acid as the CD source by combining microwave-assisted and pyrolysis methods with a size of 2–6 nm and a QY of 54%[50] for theranostic purposes. The formation of PS Ce6 in the outer layer of the CDs created a theranostic with high fluorescence due to the ROS-created singlet oxygen for PDT therapy and antitumor.[42] The CD-doped carbon nitride nanocomposite–containing polymer shows high ROS created under light illumination as a PS for anticancer therapy.[72]

7 | CONCLUSION AND FUTURE PROSPECTS

The atomic state occurred in the bandgap when photon (hv) was absorbed for producing the reactive oxide, which is important for anticancer therapy and PDT. Oxidation in the surface state increased when the bandgap decreased, which affected the number of reactive oxides produced. The intermediate radicals produced were OH*, CO_3^{-}*, and O_2^{-}* and reacted with CDs produced from H_2O_2 or mixing system with HCO_3^{-} to generate positively (CDs^{+}*) or negatively (CDs^{-}*) using strong luminescence emission when the excited state of positive or negative (CDs*) returned to ground state. The radicals produced are important for anticancer therapy and PDT. This paper also describes the characteristics of CDs from various sources that are synthesized using various methods. There are two methods: the bottom-up approach consists of hydrothermal method, microwave method, and pyrolysis, and top-down approach consists of ultrasonic method, laser ablation, and chemical oxidation.

Some studies reported the design of CDs with high ROS, high sensitivity, and selectivity to find an effective strategy based on various analyses. The traditional CDs are environment friendly and biocompatible and have broader excitation spectra, better photostability, size-dependent emission wavelength, higher QY, and efficient transfer energy. The CDs, especially those that are metal free, have the potential to develop high and effective ROS systems. In general, there is still great demand for developing high ROS CDs; designing novel CDs with highly improved sensitivity and selectivity to produce ROS is a challenge for PDT and anticancer therapy. More interesting studies in the future may focus on several areas:

- Develop new methods is needed for producing high-stability multicolor fluorescence and physical properties of CDs for reduced recombination of charge consequently high ROS produced.
- Some preparation methods are more complicated for reproducibility; therefore, research needs to be done to develop easy mass production methods with high-stable multicolor fluorescence.
- Research needs to be done for purification and functionality of the CDs to increase their QY for anticancer therapy and PDT.
- Studies CDs-based should be extended from the laboratory scale (in vitro) to the clinical trial using animals (in vivo) for therapy as anticancer and PDT therapy.

ACKNOWLEDGMENT

We would like to thank the Material and Energy lab members for their helpful discussion and in improving the quality of every figure.

DECLARATION OF INTEREST

The authors declare that they have no known competing financial or personal relationship that could have appeared to influence the work reported in this paper.

AUTHOR CONTRIBUTIONS

Nurul Mutmainnah Amal was involved in conceptualization, methodology, investigation, data curation, formal analysis, visualization, writing of the original draft, and writing—review and editing. Muhandis Shiddiq assisted with methodology, investigation, data curation, formal analysis, visualization, writing of the original draft, and writing—review and editing. Bidayatul Armynah contributed to methodology, investigation, formal analysis, and writing—review and editing. Dahlang Tahir was involved in conceptualization, supervision, writing of the original draft, and writing—review and editing.

DATA AVAILABILITY STATEMENT

The data used in the present study are available from the corresponding author on reasonable request.

ORCID

Dahlang Tahir https://orcid.org/0000-0002-8241-3604

REFERENCES

[1] V. Georgakilas, J. Perman, J. Tucek, R. Zboril, *Chem. Rev.* **2015**, *115*, 4744.
[2] F. Arcudi, L. Đorđević, M. Prato, *Acc. Chem. Res.* **2019**, *52*, 2070.
[3] A. Cayuela, M. Soriano, L. Carrillo-Carrión, M. Valcárcel, *Chem. Commun.* **2016**, *52*, 1311.
[4] G. A. Hutton, B. C. Martindale, E. Reisner, *Chem. Soc. Rev.* **2017**, *46*, 6111.
[5] N. Durán, M. B. Simões, A. C. M. de Moraes, W. J. Fávaro, A. B. Seabra, *J. Biomed. Nanotechnol.* **2016**, *12*, 1323.
[6] R. Atchudan, T. N. Edison, M. Shanmugam, S. Perumal, T. Somanathan, Y. R. Lee, *Physica E* **2020**, *126*, 114417.

[7] F. Radnia, N. Mohajeri, N. Zarghami, *Talanta* **2019**, *209*, 120547.
[8] B. Gayen, S. Palchoudhury, J. Chowdhury, *J. Nanomater.* **2019**, *1*, 19.
[9] M. K. Kumawat, M. Thakur, R. B. Gurung, R. Srivastava, *ACS Sustain. Chem. Eng.* **2017**, *5*, 1382.
[10] J. Zhou, C. Booker, R. Li, X. Zhou, T. K. Sham, X. Sun, Z. Ding, *J. Am. Chem. Soc.* **2007**, *129*, 744.
[11] X. Xu, R. Ray, Y. Gu, H. J. Ploehn, L. Gearheart, K. Raker, W. A. Scrivens, *J. Am. Chem. Soc.* **2004**, *126*, 12736.
[12] H. Zhu, X. Wang, Y. Li, Z. Wang, F. Yang, X. Yang, *Chem. Commun.* **2009**, *34*, 5118.
[13] S. Lim, Y. W. Shen, Z. Gao, *Chem. Soc. Rev.* **2015**, *44*, 362.
[14] T. Yuan, T. Meng, P. He, Y. Shi, Y. Li, X. Li, S. Yang, *J. Mater. Chem.* **2019**, *7*, 6820.
[15] H. Liu, J. Ding, K. Zhang, L. Ding, *TrAC Trends Anal. Chem.* **2019**, *118*, 315.
[16] H. Ding, X. H. Li, X. B. Chen, J. S. Wei, X. B. Li, H. M. Xiong, *J. Appl. Phys.* **2020**, *127*(23), 231101.
[17] A. Rakshit, S. S. Meenakshi, B. Surbhi, C. A. Suresh, *Emerging Green Chem. Technol.* **2018**, *135*, 175.
[18] S. Hariganesh, S. Vadivel, D. Maruthamani, S. Rangabhashisyam, *Detect. Treat.* **2020**, *279*, 304.
[19] Z. Lin, W. Xue, H. Chen, J.-M. Lin, *Anal. Chem.* **2011**, *83*, 8245.
[20] V. B. Kumar, Z. Porat, A. Gedanken, *Nanomaterials* **2022**, *12*, 898.
[21] D. M. Wang, K. L. Lin, C. Z. Huang, *Luminescence* **2018**, *34*, 4.
[22] M. Amjadi, J. L. Manzoori, T. Hallaj, *JOL* **2015**, *158*, 160.
[23] C. Xia, S. Zhu, T. Feng, M. Yang, B. Yang, *Adv. Sci. New.* **2019**, *6*, 1901316.
[24] Y. P. Sun, B. Zhou, Y. Lin, W. Wang, K. A. S. Fernando, P. Pathak, S. Y. Xie, *J. Am. Chem. Soc.* **2006**, *128*, 7756.
[25] H. Ding, J. S. Wei, P. Zhang, Z. Y. Zhou, Q. Y. Gao, H. M. Xiong, *Photoluminescent Carbon Dots.* **2018**, *14*, 1800612.
[26] S. Wang, S. H. Wu, W. L. Fang, X. F. Guo, H. Wang, *Dyes Pigm.* **2019**, *164*, 7.
[27] B. Hu, K. Wang, L. Wu, S. H. Yu, M. Antonietti, M. M. Titirici, *Adv. Mater.* **2010**, *22*, 7.
[28] Z. C. Yang, X. Li, J. Wang, *Carbon.* **2011**, *49*, 5207.
[29] V. Strauss, J. T. Margraf, C. Dolle, B. Butz, T. J. Nacken, J. Walter, D. M. Guldi, *J. Am. Chem. Soc.* **2014**, *136*, 17308.
[30] M. Jayanthi, S. Megarajan, S. B. Subramaniyan, R. Kamlekar, V. Anbazhagan, *J. Mol. Liq.* **2019**, *278*, 175.
[31] V. N. Mehta, S. S. Chettiar, J. R. Bhamore, S. K. Kailasa, R. M. Patel, *J. Fluoresc.* **2016**, *27*, 111.
[32] X. Wang, T. Gao, M. Yang, J. Zhao, F. L. Jiang, Y. Liu, *New J. Chem.* **2019**, *1*, 10.
[33] M. A. Farzin, H. Abdoos, *Talanta* **2021**, *224*, 121828.
[34] P. Devi, S. Saini, K. H. Kim, *Biosens. Bioelectron.* **2019**, *141*, 111158.
[35] M. Y. Ubani, Z. Charles Ahamefula, N. B. Sulaiman, M. Y. Ibarahim, O. Ibrahim, *J. Mod. Educ. Rev.* **2011**, *1*, 63.
[36] H. Li, X. He, Y. Liu, H. Huang, S. Lian, S. T. Lee, Z. Kang, *Carbon* **2011**, *49*, 605.
[37] M. Tsai, S. Bai, R. Chen, *Carbohydr. Polym.* **2008**, *71*, 448.
[38] Z. Feng, K. H. Adolfsson, Y. Xu, H. Fang, M. Hakkarainen, M. Wu, *Sustain. Mater. Technol.* **2021**, *29*, e00304.
[39] Z. Gao, M. Liu, K. Xu, M. Tang, X. Lin, X. Ren, S. Hu, *Anal. Methods* **2020**, *1*, 6.
[40] B. Yao, H. Huang, Y. Liu, Z. Kang, *Trends Chem* **2019**, *1*, 235.
[41] Y. Shao, C. Zhu, Z. Fu, K. Lin, Y. Wang, Y. Chang, L. Han, H. Yu, F. Tian, *J. Nanopart. Res.* **2020**, *22*, 1.
[42] P. Huang, J. Lin, X. Wang, Z. Wang, C. He, M. Zhang, X. Chen, *Adv. Mater.* **2012**, *24*, 5104.
[43] A. Sciortino, A. Cannizzo, F. Messina, *Carbon Nanodots: J. Carbon Res.* **2018**, *4*, 67.
[44] D. Reyes, M. Camacho, M. Camacho, M. Mayorga, D. Weathers, G. Salamo, A. Neogi, *Nanoscale Res. Lett.* **2016**, *11*, 1.
[45] J. L. Wilbrink, C. C. Huang, K. Dohnalova, J. M. J. Paulusse, *Faraday Discuss.* **2020**, *222*, 149.
[46] Z. L. Wu, Z. X. Liu, Y. H. Yuan, *J. Mater. Chem. B* **2017**, *5*, 3794.
[47] N. Gaponik, D. V. Talapin, A. L. Rogach, K. Hoppe, E. V. Shevchenko, A. Kornowski, H. Weller, *J. Phys. Chem. B* **2002**, *106*, 7177.
[48] L. Y. Meng, B. Wang, M. G. Ma Meng, *Mater. Today Chem.* **2016**, *1-2*, 63.
[49] A. B. Bourlinos, G. Trivizas, M. A. Karakassides, M. Baikousi, A. Kouloumpis, D. Gournis, S. Couris, *Carbon* **2015**, *83*, 173.
[50] Q. Wang, C. Zhang, G. Shen, H. Liu, H. Fu, D. Cui, *J. Nanobiotechnol.* **2014**, *12*, 58.
[51] H. Liu, Q. Wang, G. Shen, C. Zhang, C. Li, W. Ji, D. Cui, *Nanoscale Res. Lett.* **2014**, *9*, 397.
[52] Q. Jia, X. Zheng, J. Ge, W. Liu, H. Ren, S. Chen, P. Wang, *J. Colloid Interface Sci.* **2018**, *526*, 302.
[53] Y. F. Wu, H. C. Wu, C. H. Kuan, C. J. Lin, L. W. Wang, C. W. Chang, T. W. Wang, *Sci. Rep.* **2016**, *6*, 1.
[54] S. L. D'souza, S. S. Chettiar, J. R. Koduru, S. K. Kailasa, *Optik* **2018**, *158*, 893.
[55] A. Seshadri Reddy, V. G. Vo, S. S. A. An, J. Kim, *ACS Appl. Bio Mater.* **2020**, *1*, 43.
[56] Y. Shao, C. Zhu, Z. Fu, K. Lin, Y. Wang, Y. Chang, F. Tian, *J. Nanopart. Res.* **2020**, *22*, 8.
[57] J. Luo, H. Kong, M. Zhang, J. Cheng, Z. Sun, W. Xiong, H. Qu, *J. Biomed. Nanotechnol.* **2019**, *15*, 151.
[58] V. J. Sawant, S. R. Bamane, D. G. Kanase, S. B. Patil, J. Ghosh, *RSC Adv.* **2016**, *6*, 66745.
[59] F. A. Khan, N. Lammari, A. S. Muhammad Siar, K. M. Alkhater, S. Asiri, S. Akhtar, A. Elaissari, *Nanomedicine* **2020**, *15*, 969.
[60] M. Z. Fahmi, A. Haris, A. J. Permana, D. L. Nor Wibowo, B. Purwanto, Y. L. Nikmah, A. Idris, *RSC Adv.* **2018**, *8*, 38376.
[61] A. Ray Chowdhuri, S. Tripathy, C. Haldar, S. Roy, S. K. Sahu, *J. Mater. Chem. B* **2015**, *3*, 9122.
[62] X. Zhao, T. Qi, M. Yang, W. Zhang, C. Kong, M. Hao, J. Jiang, *Nanomedicine* **2020**, *15*, 677.
[63] T. Feng, X. Ai, G. An, P. Yang, Y. Zhao, *ACS Nano* **2016**, *10*, 4410.
[64] P. Das, S. Ganguly, T. Agarwal, P. Maity, S. Ghosh, S. Choudhary, N. C. Das, *Mater. Chem. Phys.* **2019**, *237*, 121860.
[65] S. Şimşek, A. A. Şüküroğlu, D. Yetkin, B. Özbek, D. Battal, R. Genç, *Sci. Rep.* **2020**, *10*, 13880.
[66] K. Y. Choi, K. H. Min, Y. H. Yoon, K. Kim, J. H. Park, I. C. Kwon, K. Choi, S. Y. Jeong, *Biomaterials* **2011**, *32*, 1880.
[67] S. Sarkar, D. Gandla, Y. Venkatesh, P. R. Bangal, S. Ghosh, Y. Yang, S. Misra, *Chem. Phys.* **2016**, *18*, 21278.
[68] S. Parveen, R. Misra, S. K. Sahoo, *Nanomed. Nanotechnol. Biol. Med.* **2012**, *8*, 147.
[69] S. S. Liang, L. Qi, R. L. Zhang, M. Jin, Z. Q. Zhang, *Sens. Actuators B* **2017**, *244*, 585.
[70] C. Dias, N. P. Vasimalai, M. Sárria, I. Pinheiro, V. Vilas-Boas, J. Peixoto, B. Espiña, *Nanomaterials* **2019**, *9*, 199.
[71] M. Tomeh, R. Hadianamrei, X. Zhao, *Int. J. Mol. Sci.* **2019**, *20*, 1033.
[72] E. S. M. Cutrim, A. A. M. Vale, D. Manzani, H. S. Barud, E. Rodríguez-Castellón, A. P. S. A. Santos, A. C. S. Alcântara, *Mater. Sci. Eng. C* **2021**, *120*, 111781.
[73] D. W. Zheng, B. Li, C. X. Li, J. X. Fan, Q. Lei, C. Li, X. Z. Zhang, *ACS Nano* **2016**, *10*, 8715.
[74] T. J. Dougherty, C. J. Gomer, B. W. Henderson, G. Jori, D. Kessel, M. Korbelik, Q. Peng, *JNCI J. Natl. Cancer Inst.* **2012**, *90*, 889.
[75] R. Vankayala, K. C. C. Hwang, *Adv. Mater.* **2018**, *30*, 1706320.
[76] P. Huang, J. Lin, X. Wang, Z. Wang, C. Zhang, M. He, X. Chen, *Adv. Mater.* **2012**, *24*, 5104.

[77] X. Hu, S. Wang, Q. Luo, B. Ge, Q. Cheng, C. Dong, H. Bi, *Chin. Chem. Lett*. **2021**, *32*, 2287.
[78] Q. Dong, J. Li, L. Cui, H. Jian, A. Wang, S. Bai, *Colloids Surf*. **2017**, *516*, 190.
[79] K. Wang, Q. He, X. Yan, Y. Cui, W. Qi, L. Duan, J. Li, *J. Mater. Chem.* **2007**, *17*, 4018.
[80] M. Kuruppuarachchi, H. Savoie, A. Lowry, C. Alonso, R. W. Boyle, *Mol. Pharm.* **2011**, *8*, 920.
[81] M. Korbelik, *Lasers Surg. Med.* **2006**, *38*, 500.
[82] C. A. Robertson, D. H. Evans, H. Abrahamse, *J. Photochem. Photobiol. B* **2009**, *96*, 1.
[83] H. Thomsen, N. Marino, S. Conoci, S. Sortino, M. B. Ericson, *Sci. Rep.* **2018**, *8*, 9753.
[84] S. Beack, W. H. Kong, H. S. Jung, I. H. Do, S. Han, H. Kim, K. S. Kim, S. H. Yun, S. K. Hahn, *Acta Biomater.* **2015**, *26*, 295.
[85] J. Ge, M. Lan, B. Zhou, W. Liu, L. Guo, H. Wang, X. Han, *Nat. Commun.* **2014**, *5*, 1.
[86] T. A. Tabish, C. J. Scotton, D. C. Ferguson, L. Lin, A. der Veen, S. Lowry, S. Zhang, *Nanomedicine* **2018**, *13*, 1923.
[87] E. Campbell, M. T. Hasan, R. Gonzalez-Rodriguez, T. Truly, B. H. Lee, K. N. Green, A. V. Naumov, *Nanomed. Nanotechnol. Biol. Med.* **2021**, *37*, 102408.
[88] K. Kholikov, S. Ilhom, M. Sajjad, M. E. Smith, J. D. Monroe, O. San, A. O. Er, *Photodiagnosis Photodyn. Ther.* **2018**, *24*, 7.
[89] H. Fan, X. Yu, K. Wang, Y. Yin, Y. Tang, Y. Tang, X. Liang, *Eur. J. Med. Chem.* **2019**, *182*, 111620.
[90] Y. Li, X. Zheng, X. Zhang, S. Liu, Q. Pei, M. Zheng, Z. Xie, *Adv. Healthc. Mater.* **2016**, *6*, 1600924.
[91] X. Qin, J. Liu, Q. Zhang, W. Chen, X. Zhong, J. He, *Nanoscale Res. Lett*. **2021**, *16*, 1.
[92] A. A. Chen, *Nucleic Acids Res.* **2005**, *33*, 22.
[93] W. B. Tan, S. Jiang, Y. Zhang, *Biomaterials* **2007**, *28*, 1565.
[94] T. Song, Y. Qu, Z. Ren, S. Yu, M. Sun, X. Yu, X. Yu, *Int. J. Mol. Sci.* **2021**, *22*, 8106.
[95] L. Menilli, A. R. Monteiro, S. Lazzarotto, F. M. P. Morais, A. T. P. C. Gomes, N. M. M. Moura, S. Fateixa, M. A. F. Faustino, M. G. P. M. S. Neves, T. Trindade, G. Miolo, *Pharmaceutics*. **2021**, *13*, 1512.
[96] K. Szaciłowski, W. Macyk, A. Drzewiecka-Matuszek, M. Brindell, G. Stochel, *Chem. Rev.* **2005**, *105*, 2647.
[97] J. M. Dąbrowski, *Adv. Inorg. Chem.* **2017**, *70*, 343.
[98] J. J. Hu, Q. Lei, X. Z. Zhang, *Prog. Mater. Sci.* **2020**, *114*, 100685.
[99] Z. Zhou, J. Song, L. Nie, X. Chen, *Chem. Soc. Rev.* **2016**, *45*, 6597.
[100] G. Stochel, M. Brindell, W. Macyk, Z. Stasicka, K. Szaciłowski, *Chichester*. **2009**, *63*, 382.
[101] J. Hu, Y. A. Tang, A. H. Elmenoufy, H. Xu, Z. Cheng, X. Yang, *Small* **2015**, *11*, 5860.
[102] A. M. Smith, M. C. Mancini, S. Nie, *Nanotechnology* **2009**, *4*, 710.
[103] J. M. Dąbrowski, B. Pucelik, A. Regiel-Futyra, M. Brindell, O. Mazuryk, A. Kyzioł, G. Stochel, W. Macyk, L. G. Arnaut, *Coord. Chem. Rev.* **2016**, *325*, 67.
[104] S. Luo, E. Zhang, Y. Su, T. Cheng, C. Shi, *Biomaterials* **2011**, *32*, 7127.
[105] J. M. Dabrowski, L. G. Arnaut, *Photochem. Photobiol. Sci.* **2015**, *14*, 1765.
[106] L. B. Rocha, F. Schaberle, J. M. Dąbrowski, S. Simões, L. G. Arnaut, *Int. J. Mol. Sci.* **2015**, *16*, 29236.
[107] R. Saavedra, L. B. Rocha, J. M. Dąbrowski, L. G. Arnaut, *ChemMedChem* **2014**, *9*, 390.
[108] A. S. L. Derycke, P. A. M. de Witte, *Adv. Drug Deliv. Rev.* **2004**, *56*, 17.
[109] M. Mitsunaga, M. Ogawa, N. Kosaka, L. T. Rosenblum, P. L. Choyke, H. Kobayashi, *Nat. Med.* **2011**, *17*, 1685.
[110] J. R. Mourant, M. Canpolat, C. Brocker, O. Esponda-Ramos, T. M. Johnson, A. Matanock, K. Stetter, J. P. Freyer, *J. Biomed. Opt*. **2020**, *5*(2), 131.
[111] J. Frangioni, *Curr. Opin. Chem. Biol.* **2003**, *7*(5), 626.
[112] D. van Straten, V. Mashayekhi, H. de Bruijn, S. Oliveira, D. Robinson, *Cancer* **2017**, *9*(2), 19.
[113] L. Carroll, T. R. Humphreys, *Clin. Dermatol.* **2006**, *24*(1), 2.
[114] M. M. Kim, A. Darafsheh, *Photochem. Photobiol.* **2020**, *96*(2), 280.
[115] L. Brancaleon, H. Moseley, *Lasers Med. Sci.* **2002**, *17*(3), 173.
[116] K. F. Gibson, W. G. Kernohant, *Med. Eng. Technol.* **1993**, *17*(2), 51.
[117] D. Pariser, R. Loss, M. Jarratt, W. Abramovits, J. Spencer, R. Geronemus, P. Bailin, S. Bruce, *Am. Acad. Dermatol.* **2008**, *59*(4), 569.
[118] J. Hempstead, D. P. Jones, A. Ziouche, G. M. Cramer, I. Rizvi, S. Arnason, T. Hasan, J. P. Celli, *Sci. Rep.* **2015**, *5*(1), 10093.
[119] A. Erkiert-Polguj, A. Halbina, I. Polak-Pacholczyk, H. Rotsztejn, *Laser Ther.* **2016**, *18*(2), 105.
[120] C. Cantisani, G. Paolino, U. Bottoni, S. Calvieri, *Drugs Dermatol.* **2015**, *14*(11), 1349.
[121] J. P. Lacour, C. Ulrich, Y. Gilaberte, V. Von Felbert, N. Basset-Seguin, B. Dreno, C. Girard, P. Redondo, C. Serra-Guillen, I. Synnerstad, M. Tarstedt, *Acad. Dermatol. Venereol.* **2015**, *29*(12), 2342.
[122] A. Kamkaew, F. Chen, Y. Zhan, R. L. Majewski, W. Cai, *ACS Nano* **2016**, *10*, 3918.
[123] C. Zhang, K. Zhao, W. Bu, D. Ni, Y. Liu, J. Feng, J. Shi, *Chem. Int. Ed.* **2015**, *54*, 1770.
[124] X. Zou, M. Yao, L. Ma, M. Hossu, X. Han, P. Juzenas, W. Chen, *Nanomedicine* **2014**, *9*, 2339.
[125] X. Yu, X. Liu, W. Wu, K. Yang, R. Mao, F. Ahmad, X. Chen, W. Li, *Angew. Chem. Int. Ed.* **2019**, *58*, 2017.
[126] Z. M. Markovic, B. Z. Ristic, K. M. Arsikin, D. G. Klisic, L. M. Harhaji-Trajkovic, B. M. Todorovic-Markovic, V. S. Trajkovic, *Biomaterials* **2012**, *33*, 7084.
[127] M. Zhang, W. Wang, Y. Cui, X. Chu, B. Sun, N. Zhou, J. Shen, *Chem. Eng. J.* **2018**, *338*, 526.
[128] M. Zhang, W. Wang, N. Zhou, P. Yuan, Y. Su, M. Shao, F. Pan, *Carbon* **2017**, *118*, 752.

How to cite this article: N. M. Amal, M. Shiddiq, B. Armynah, D. Tahir, *Luminescence* **2022**, 1. https://doi.org/10.1002/bio.4388